Journal of Catalysis 282 (2011) 201–208

Contents lists available at ScienceDirect

Journal of Catalysis

journal homepage: www.elsevier.com/locate/jcat

Oxidative desulfurization (ODS) of organosulfur compounds catalyzed by peroxo-metallate complexes of WOx–ZrO_2: Thermochemical, structural, and reactivity indexes analyses

E. Torres-García [a,*], A. Galano [b,*], G. Rodriguez-Gattorno [c]

[a] Instituto Mexicano del Petróleo, Eje Central Norte, Lázaro Cárdenas 152, San Bartolo Atepehuacan, 07730 México DF, Mexico
[b] Departamento de Química, Universidad Autónoma Metropolitana-Iztapalapa, San Rafael Atlixco 186, Col. Vicentina, Iztapalapa, CP 09340 México DF, Mexico
[c] Departamento de Física Aplicada, CINVESTAV-IPN, Mérida, Yucatán 97310, Mexico

ARTICLE INFO

Article history:
Received 8 March 2011
Revised 27 May 2011
Accepted 13 June 2011
Available online 26 July 2011

Keywords:
Oxidative desulfurization
Tungstated zirconia
Sulfur compounds
Peroxo-metallate complexes
Density-functional theory (DFT)

ABSTRACT

An experimental and theoretical study on the relationships between oxidative reactivity, thermochemical viability, and structural requirement of the activity sites in oxidative desulfurization (ODS) process has been performed. A series of aromatic sulfur compounds and peroxo-metallate complexes of WOx–ZrO_2 with different structures have been studied. The models chosen for mimicking the catalyst correspond to surface densities of $\sim$7 W nm^{-2}. The results indicate that the ODS takes place in two consecutive stages: (i) the formation of sulfoxide and (ii) the formation of sulfone. However, a detailed analysis suggests that these stages occur in two separated steps, (a) addition and (b) elimination, involving the formation of intermediate adducts and that the elimination of sulfoxide from the site surface is the rate-determining step. The results also reveal that the thermochemical feasibility of the studied reactions depends on both: the local structure of the WOx–ZrO_2 surface and on the nature of the aromatic sulfur compound. It was found that the reactions involving dibenzothiophene (DBT) and 4,6-dimethyldibenzothiophene (46DMDBT) are the most favored reactions, while the reaction of thiophene (Th) is the least favored. Therefore, highly substituted dibenzothiophenes are the most readily oxidized species, which is in agreement with experimental evidence. An explanation to the different reactivity shown by sulfur compounds, during ODS processes, is provided.

1. Introduction

Oxidative desulfurization (ODS) is considered a promising method for ultra-deep desulfurization of fuel oils. The interest on such process is well justified since the removal of sulfur compounds from fuels is necessary for industrial and environmental reasons. Organic sulfur compounds present in diesel widely vary in structure and therefore in reactivity during catalytic hydrodesulfurization (HDS) [1,2]. In HDS, the reactivity of dibenzothiophenes dramatically decreases with the increase of methyl substitutes at the sterically hindered positions 4 and 6 [3,4]. Consequently, in deep HDS, the conversion of these substituted dibenzothiophenes strongly depend on the experimental conditions. Therefore, an important feature for application of the ODS in ultra-low-sulfur process is that its relative efficiency is different from that of HDS: DBT > 4-MDBT > 46-DMDBT > BT [4–6]. As a consequence, refractory sulfur compounds in HDS are easily removed by ODS. This makes ODS a chemical strategy with great potential to be complementary to traditional HDS for producing deeply desulfurized light oil and for reaching the environmental regulations.

In the ODS process, the organosulfur compounds are oxidized to their corresponding sulfoxides or sulfones. The process is carried out under mild conditions in the presence of a catalyst and an oxidant agent, and the oxidized sulfur compounds are subsequently removed by extraction, adsorption, distillation, or decomposition [5–8]. The main advantage of ODS is that sulfur compounds can be removed without using a hydrogen atmosphere, at relatively low temperatures and at atmospheric pressure. However, from technologic points of view, the development and implementation of the ODS alternative for ultra-low-sulfur processes are still a challenge for both academia and industry.

An extremely important point relevant to the ODS process is related to the catalytic material, particularly to the structural requirements of the active sites and its relationships with the catalytic efficiency. Consequently, a large variety of studies have been carried out on oxidizing sulfur compounds with different catalysts and under different conditions [2,3,9–17]. Regardless of the numerous works on ODS, considering both heterogeneous and

* Corresponding authors.
E-mail addresses: etorresg@imp.mx (E. Torres-García), agalano@prodigy.net.mx (A. Galano).

0021-9517/$ - see front matter © 2011 Elsevier Inc. All rights reserved.
doi:10.1016/j.jcat.2011.06.010

homogeneous systems, little attention has been paid to systematic studies on the influence of the structural characteristics of the peroxo-complexes surface on the thermochemical feasibility and the relative reactivity of organosulfur compounds during ODS process. The researches in this field are difficult, in part due to the fact that it is very complicated to separate the different factors and also because they presume establishing the influence of each component during the process. Another reason is the absence of systematic studies on the chemical nature of sulfur compounds and on possible relationships between such nature and the characteristics of the reactive sites on the catalyst surface.

In correspondence, the purpose of this work is to provide an analysis of the relationships between the structural requirements of the active sites on the catalyst's surface, the nature of sulfur compounds, and the thermodynamic feasibility of the key steps in the ODS process. To that purpose, a combined experimental and theoretical study on different sulfur compounds has been realized. For the experimental study, four organosulfur compounds have been used. They are thiophene (Th), benzothiophene (BT), dibenzothiophene (DBT), and 4,6-dimethyldibenzothiophene (46DMDBT) and were selected because they are the most frequents in fuels. For the theoretical study, a larger series of sulfur compound have been chosen, in order to search for generalizations regarding structure–reactivity relationships. They are thiophene (Th), benzothiophene (BT), dibenzothiophene (DBT), 2,5-dimethylthiophene (25DMT), 2-methylbenzothiophene (2MBT), 4-methylbenzothiophene (4MBT), 2,4-dimethylbenzothiophene (24DMBT), and 4,6-dimethyldibenzothiophene (46DMDBT). Various reactivity indexes have been analyzed to that purpose: hardness (η), electrophilicity (ω), electroaccepting power (ϖ^+), and electrodonating power (ϖ^-). They have been used to provide a viable explanation to the experimental reactivity of different organosulfur compounds during the ODS process.

2. Experimental

2.1. Catalyst preparation

High-surface-area $ZrO_{2-x}(OH)_{2x}$ (320 m^2/g) was prepared by precipitation from zirconium oxychloride solutions with ammonia as previously described [18,19]. The precipitate was filtrated, washed repeatedly by re-dispersion with a NH_4OH solution (pH 10) until the elimination of Cl^-, and then dried at 383 K for 24 h. Subsequently, $ZrO_{2-x}(OH)_{2x}$ was impregnated with an ammonium metatungstate solution, adjusted to pH 10 with ammonia, as reported in Ref. [20]. After drying at 383 K for 24 h, the samples were treated in flowing dry air for 3 h at 1073 K. The stabilized specific surface area of WO*x*–ZrO_2 in calcined samples was about 50 m^2/g and pore size of about 6.2 nm. WO*x* surface densities used in this study was of ~7 W nm^{-2}.

2.2. Catalytic test

A synthetic diesel was prepared with heptane (C_7H_{16}, 99.0 mol.%) as solvent, and 140 S ppmw of thiophene (Th, 99+%), 186 S ppmw of benzothiophene (BT, 98%), 222 S ppmw of dibenzothiophene (DBT, 98%), and 173 S ppmw of 4,6-dimethyldiebenzothiophene (46DMDBT, 97%) were used as the sulfides. Hydrogen peroxide (aqueous solution, 30 wt.%) and acetonitrile (CH_3CN, 99.93 mol.%) were used as oxidizing agent and as extraction solvent, respectively. All the reagents used in this study are commercially available (Sigma/Aldrich).

In an typical run, the solid catalyst, 0.1 g of WO*x*–ZrO_2 catalyst was suspended under vigorous stirring (1200 rpm) in a mixture containing 50 mL synthetic diesel, solvent (model fuel/solvent ratios 1:1, v/v), and oxidizing hydrogen peroxide was added in H_2O_2/S ratios 10:1. A Robinson–Mahoney reactor was used in order to perform the chemical reactions. The oxidation was carried out at 333 K, and the samples were collected from the reaction mixture during the reaction at time intervals. Both oil and polar phase with sulfides were analyzed by GC-HP6890 equipped with a HP-5 capillary column (30 m × 0.25 mm, 0.32 μm film thickness) and FPD/FID detector. The hydrogen peroxide, presented during the reaction, was measured by standard iodometric titration.

2.3. Conversion of sulfur

The data gathered from the experiments were used to calculate the removal fraction (S_t) of sulfides as follows:

$$S_t = \left(\frac{C_0 - C_t}{C_0}\right)$$

where C_0 is the initial concentration of sulfides in the heptane solution and C_t is the sulfides concentration of the oil phase after reaction time (t).

2.4. Oxidation of different organosulfur compounds

The oxidative reaction of each sulfur compound follows first-order kinetics, according to previous reports obtained with aromatic sulfur compounds on solid catalysts [5,21–24]. Due to the large excess of hydrogen peroxide, the concentration of this compound remains practically constant. Therefore, the following equation applies: $\ln(C_t/C_0) = -kt$, where $k = A\exp(-E/RT)$, A is the pre-exponential factor, E the apparent activation energy, R and T are the gas constant and reaction temperature, respectively.

2.5. Computational details

The calculations were performed using Gaussian 03 [25] package of programs. Geometry optimizations have been performed using the generalized gradient approximation (GGA), without any symmetry constraints. The Perdew and Wang's 1991 functional [26] (PW91) was used for exchange and correlation potentials. We have used the Dunning/Huzinaga valence double-zeta D95 V [27] basis set for O, C, N, and H atoms and the Stuttgart/Dresden [28–30] relativistic effective core potential (ECP) for W and Zr. Frequency calculations were carried out for all the studied systems at the same level of theory. Thermodynamic corrections at 333 K were included in the calculation of the relative energies. The stationary points were first modeled in gas phase (vacuum), and solvent effects were included *a posteriori* by single-point calculations using polarizable continuum model, specifically the integral-equation-formalism (IEF-PCM) [31–34] at the same level of theory, with acetonitrile as solvent to mimic the experimental conditions. For all the modeled paths, the solute cavity was computed using atomic radii from the universal force field (RADII = UFF), which assigns individual spheres to H atoms (explicit hydrogens). Different levels of theory were tested for the calculation of reactivity indexes of the sulfur compounds, and the reported values are those obtained at B3LYP/6-311++G(d,p) level of theory.

The rate constants (k) were calculated using Conventional Transition State Theory (TST) [35–37] and 1 M standard state as:

$$k = \frac{k_B T}{h} e^{-(\Delta G^{\neq})/RT} \quad (1)$$

where k_B and h are the Boltzmann and Planck constants and $\Delta G^{\neq}$ is the Gibbs free energy of activation.

Some of the calculated rate constants (k) are in the diffusion-limit. Accordingly, the apparent rate constant (k_{app}) cannot be directly obtained from TST calculations. In the present work, we have used the Collins–Kimball theory for that purpose [38]:

$$k_{app} = \frac{k_D k_{act}}{k_D + k_{act}} \quad (2)$$

where k_{act} is the thermal rate constant, obtained from TST, and k_D is the steady-state Smoluchowski [39] rate constant for an irreversible bimolecular diffusion-controlled reaction:

$$k_D = 4\pi R D_{AB} N_A \quad (3)$$

where R denotes the reaction distance, N_A is the Avogadro number, and D_{AB} is the mutual diffusion coefficient of the reactants. However, in this study, D_{AB} has been assumed equal to D_A (where A represents the sulfur compound) since the catalyst is not expected to diffuse. D_A has been estimated from the Stokes–Einstein approach [40]:

$$D_A = \frac{k_B T}{6\pi\eta a} \quad (4)$$

where k_B is the Boltzmann constant, T is the temperature, η denotes the viscosity of the solvent, in our case acetonitrile ($\eta = 4.41 \times 10^{-4}$ Pa s), and a the radius of the solute ($a_{DBT} = 8.15$ Å).

3. Results and discussion

3.1. Catalytic reaction

On the basis of previous works [18,41] and in order to establish the relationships between the structural characteristics of the reactive sites on the catalyst surface and the thermochemical feasibility of the reactions of different organosulfur compounds in oxidative desulfurization, a model system with WOx–ZrO_2 as catalyst, acetonitrile as extraction solvent, and hydrogen peroxide as oxidant has been chosen. Recently, we reported that oxidative efficiency (expressed as % sulfur removed/W atom nm^{-2} min^{-1}) of the WOx–ZrO_2 system (per W atom) for ODS of DBT increases with increasing WOx surface density up to a maximum of ~7 W nm^{-2} (see Fig. 1). This value represents the point where the local coordination and polymerization degree of the WOx domains, in mutual cooperation, produce a maximum number of Brönsted sites per surface unit, promoting the addition of OOH groups. The study also revealed that the combined presence of Lewis and Brönsted sites energetically favored the formation of peroxo-metallate and that dimeric species are adequate to describe the properties of the peroxo-complexes surface from chemical and catalytic points of view [19,42]. Clearly, this analysis showed that to obtain an adequate balance between local coordination, polymerization degree of the WOx domains, and high-density surface of Brönsted acid sites, the WOx–ZrO_2 system requires an exact control of surface acid properties.

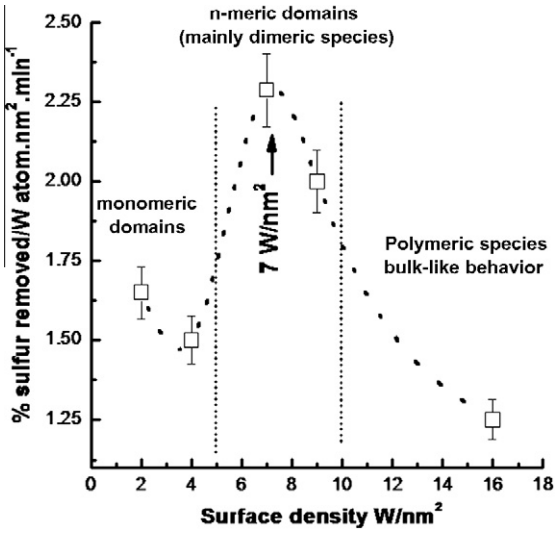

Fig. 1. Catalytic efficiency as function of WOx surface density (W nm^{-2}) [42].

Accordingly, our catalytic study focuses on the zone where the oxidative efficiency of the reaction reaches its maximum (WOx surface density ~7 W nm^{-2}). Oxidative removals for different organic sulfur compounds as a function of reaction time over WOx–ZrO_2 at 333 K are shown in Fig. 2A. The maximum conversion is obtained for DBTs and BT after 60 min of reaction. By contrast, the reaction of Th is the least favored. The oxidative reactivity, evaluated as oxidation rate constants (k) (Fig. 2B), decreased according to the following order: DBT > 46DMDBT > BT ≫ Th, in good agreement with theoretical and experimental previous reports [5,10,11,43,44]. The oxidized products of DBTs and BT are the corresponding sulfones, while sulfoxides were not detected as products. In the case of thiophene, the reaction yielded H_2SO_4 and thiophene sulfoxide, but thiophene sulfone was not detected. This can be explained based on the results of our calculations. Among all the studied sulfur compounds, only in the case of thiophene, the structure of the addition product formed in stage 2 (a) shows a noticeable weakening of the C–S bonds. Moreover, this feature is also present in the thiophene sulfone. This structural characteristic supports the possibility of the sulfone decomposition yielding SO_2, when the ODS process involves thiophene. Under oxidation conditions, it can evolve into SO_3. Additionally, in the presence of water, these sulfur oxides can be converted to the corresponding acids. These results suggest that the products arising from oxidation reactions would be dependent on the nature of the reacting sulfur compound.

The results clearly indicate that DBT and 46DMDBT are the most readily oxidized species, suggesting that under the experimental condition used in this study, the order of reactivity can be related to the electron density on the sulfur atoms in these compounds [5,43,44]. Apparently, the number of rings and the number of methyl groups both increase the oxidative reactivity of these compounds. This is probably because the methyl groups in the aromatic rings act as electron donors. This behavior enhances the electron density on the sulfur atom, promoting the catalytic reaction.

Therefore, to get deeper insight, a detailed study of the reaction steps is crucial to rationalize the relative oxidative reactivity of the series of organosulfur compounds found in fuels. To that purpose, a theoretical systematic study was accomplished focusing on the thermochemical viability of such process through estimations of spontaneity. Consequently, the relevant points would be those corresponding to the initial and final states. This approach is supported by the Hammond postulate and the Bell–Evans–Polanyi principle.

3.2. Theoretical considerations

3.2.1. Thermochemical viability of the ODS reactions

According to the experimental results shown in the Fig. 1, all models in this study correspond to the zone where catalytic reaction reaches its maximum (~7 W nm^{-2}). Six different arrangements have been chosen to mimic the local surface of the WOx–ZrO_2 catalyst. The structures used to model the peroxo-complexes correspond to those previously proposed as the most likely products arising from peroxidation of WOx–ZrO_2 surfaces [42] and are provided as Supporting Information (Fig. 1S). The original WOx–ZrO_2 structures correspond to tetrahedral W, with different degrees of surface hydroxylation [19,42]. Their ODS reactions with eight aromatic sulfur compounds have been modeled. The studied sulfur compounds are thiophene (Th), benzothiophene (BT), dibenzothiophene (DBT), 2,5-dimethylthiophene (25DMT), 2-methylbenzothiophene (2MBT), 4-methylbenzothiophene (4MBT), 2,4-dimethylbenzothiophene (24DMBT), and 4,6-dimethyldibenzothiophene (46DMDBT).

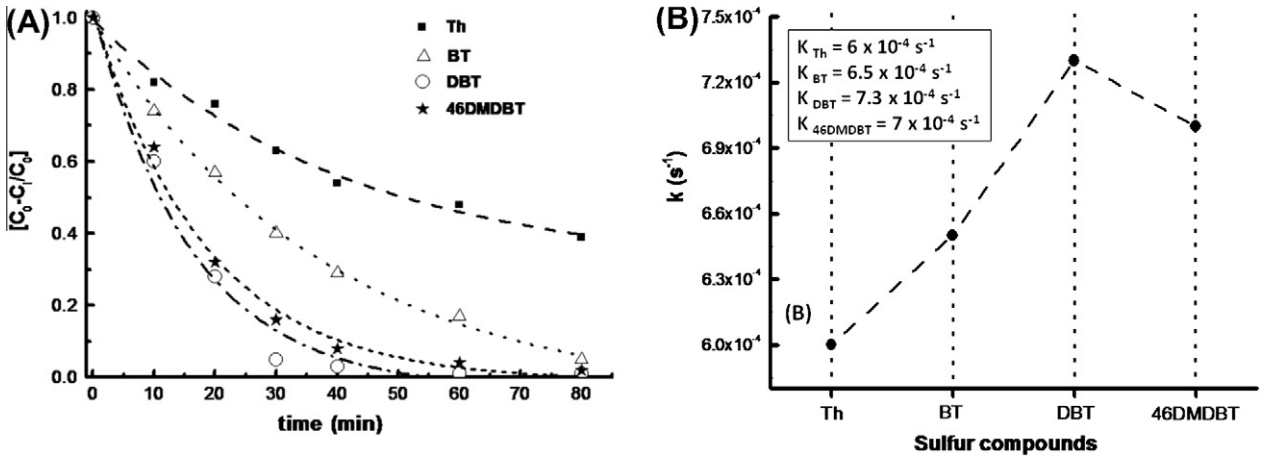

Fig. 2. (A and B) ODS of different sulfur compounds over WO*x*–ZrO_2 catalyst as a function reaction time. (B) Rate constants (*k*) of different sulfur compounds, evaluated as oxidation rate constants (*k*). Reaction conditions: WO*x*–ZrO_2, 0.1 g; H_2O_2/S = 10:1; model fuel/acetonitrile ratios 1:1 v/v; 333 K and 101 kPa.

The ODS is proposed to take place in two consecutive stages, the first one leading to the formation of sulfoxide and the second one yielding sulfone:

Stage 1: POO + XS → PO + XSO
Stage 2: POO + XSO → PO + XSO_2

where POO represents the peroxo-metallate, XS the aromatic sulfur compound, XSO the sulfoxide, and XSO_2 the sulfone. The direct mechanism yielding the XSO_2 compounds was found to be largely endergonic (by more than 100 kcal/mol), and therefore, it was ruled out.

The enthalpies and Gibbs free energies of reactions of the ODS stages are reported in Tables 1 and 2. Peroxo-complexes with structures B1 and Eb were found to be those leading to the most thermochemically favored reactions, for all the modeled sulfur compounds. Their structures are shown in Fig. 3. In general, the thermochemical feasibility of the second stage of reaction was found to be larger than that of the first one. Therefore, the latter seems to be the key stage for the success of the ODS process.

The first stage of reactions involving structures B2, Ea, and Fa (Figure 1S) was found to be endergonic for all the studied sulfur compounds. This suggests that such kinds of sites are unlike to participate in the ODS reactions. When the peroxo-complex corresponds to structure D (Figure 1S), most of the first stages of reaction are predicted to be endergonic, with the exceptions of the reactions involving DBT and 46DMDBT. In fact, a general trend was found for the first stage of reaction with respect to the reacting sulfur compound, that is DBT and 46DMDBT were found to be the ones involved in the most thermochemically favored reactions. Th and 25DMT, on the other hand, were found to be the sulfur compounds leading to the least thermochemically favored first stages of the ODS reactions. These considerations are agreement with our experimental result.

3.2.2. Kinetics analysis and mechanism of reaction

So far, stages 1 and 2 have been considered to take place as elementary reactions. However, another alternative is also possible that each stage actually takes place in two steps, involving the formation of intermediate adducts (Fig. 4). According to this hypothesis, the ODS mechanism would become:

Stage 1:
Step 1a: POO + XS → POO-SX
Step 1b: POO-SX → PO + XSO
Stage 2:
Step 2a: POO + XSO → POO-S(O)X
Step 2b: POO-S(O)X → PO + XSO2

Within this scheme, *step 1a* represents the addition of the sulfur compound to the peroxo-metallate, *step 1b* is the elimination of the sulfoxide, *step 2a* the addition of the sulfoxide to another peroxo site, and *step 2b* the elimination of the sulfone.

The four steps scheme has been modeled for all the studied sulfur compounds and cluster B1. The corresponding Gibbs free energies of reaction are reported in Table 3. As these values show the

Table 1
Enthalpies of reaction for the OOS process, in kcal/mol at 333 K.

	Th	25DMT	BT	2MBT	4MBT	DBT	24DMBT	46DMDBT
Stage 1								
B1	171	−0.60	−1.29	−1.42	−1.83	−5.26	−2.05	−8.68
B2	1509	9.50	8.80	8.68	8.26	4.83	8.04	4.70
D	9.18	3.58	2.89	2.76	2.34	−1.09	2.12	−1.20
Ea	1421	621	5.51	5.39	4.97	1.54	4.75	3.83
Eb	−0.69	−3.97	4.66	4.79	−5.20	−8.64	−5.42	−11.08
Fa	1673	11 12	10.42	10.30	9.88	6.45	9.66	6.34
Stage 2								
B1	−1207	−11.80	−9.62	−10.22	−9.91	−9.78	−10.35	14.14
B2	131	−1.71	0.47	−0.13	0.18	0.31	−0.26	−0.77
D	4.60	−7.62	−5.44	−6.04	−5.74	−5.60	−6.17	−6.67
Ea	043	−4.99	−2.82	−3.42	−3.11	−2.98	−3.55	−1.64
Eb	−1448	−15.17	−12.99	−13.59	−13.28	−13.15	−13.72	16.55
Fa	294	−0.08	2.09	1.50	1.80	1.94	1.36	0.87

Table 2
Gibbs free energies of reaction for the ODS process, in kcal/mol at 333 K.

	Th	25DMT	BT	2MBT	4MBT	DBT	24DMBT	46DMDBT
Stage 1								
Bl	3.59	−2.05	−2.84	−2.77	−3.27	−6.80	−3.43	−6.60
B2	15.19	9.56	8.77	8.83	8.34	4.80	8.18	5.01
D	8.48	2.85	2.06	2.12	1.63	−1.91	1.47	−1.70
Ea	11.31	5.67	4.88	4.94	4.45	0.91	4.29	1.12
Eb	2.86	−2.77	−3.56	−3.50	−3.99	−7.53	−4.15	−7.72
Fa	15.69	10.05	9.26	9.33	8.83	5.29	8.67	5.50
Stage 2								
Bl	−9.18	−12.57	−10.14	−10.99	−10.79	−10.27	−11.72	−11.67
B2	2.43	−0.96	1.46	0.62	0.82	1.34	0.11	−0.06
D	−4.28	−7.67	2.5	−6.09	−5.89	−5.37	−6.82	−6.77
Ea	−1.46	−4.85	−2.42	−3.27	−3.07	−2.55	−400	−3.95
Eb	−9.90	−13.29	−10.87	−11.71	−11.51	−10.99	−1244	−12.39
Fa	2.92	−0.47	1.96	1.11	1.31	1.83	0.38	0.43

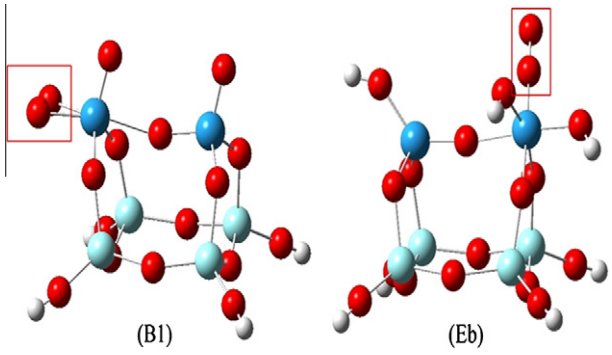

Fig. 3. Structures of the peroxo-metallates B1 and Eb. The boxes highlight the peroxo-sites. (red = O, dark blue = W, light blue = Zr, white = H). (For interpretation of the references to colour in this figure legend, the reader is referred to the web version of this article.)

addition steps are systematically more favored than the elimination steps. Moreover, the elimination of the sulfoxide was found to be endergonic for all the studied systems. This means that this is a reversible step, for which the direct reaction is not thermochemically favored. However, the products from *step 1b* can still react further if the following step (*2a*) is sufficiently exergonic to provide a driving force and if its barrier is low. In such cases, the small amounts of sulfoxide formed from *step 1b* would be consumed though *step 2a* causing the equilibrium to evolve toward the formation of more sulfoxide, and the overall process would proceed slowly. Accordingly, *step 1b* (the elimination of sulfoxide from the catalyst surface) is proposed to be the rate-determining step.

To test this hypothesis, kinetic calculations have been performed for the ODS process of DBT, using the B1 cluster to model the catalyst. The values of the Gibbs free energy of activation and rate constants for the four steps are provided in Table 4. These values show that the barriers of the addition steps (*1a* and *2a*) are significantly lower than those of the elimination steps (*1b* and *2b*). Moreover, the highest barrier corresponds to *Step 1b* (Fig. 5). According to the calculated rate constants, the addition steps are predicted to be diffusion controlled. The smallest rate constant corresponds to *Step 1b*, supporting the

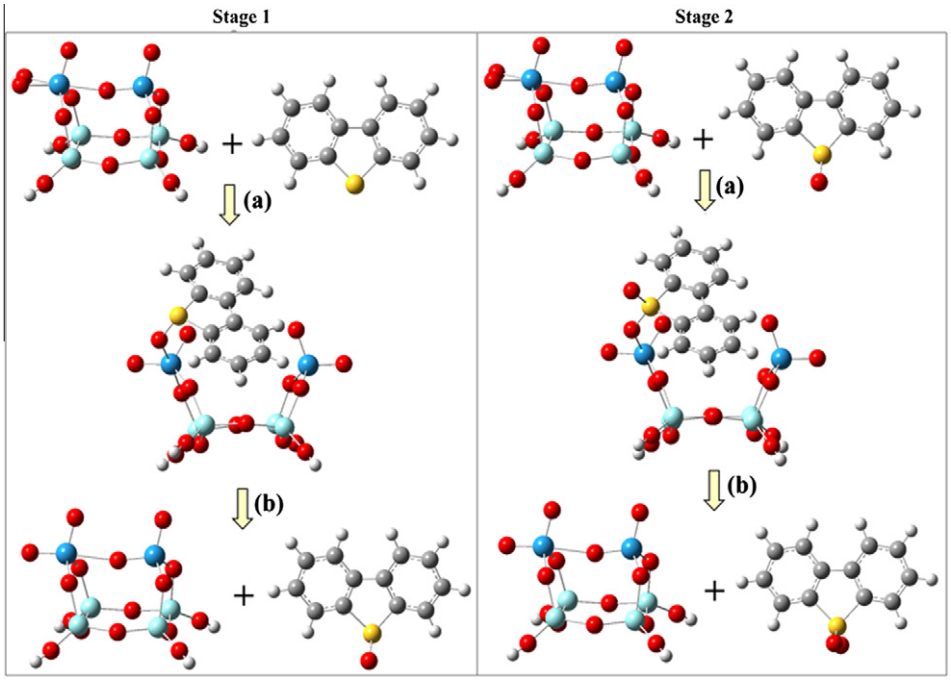

Fig. 4. Reaction steps of the ODS process, exemplified for the B1 + DBT. (red = O, dark blue = W, light blue = Zr, white = H, gray = C, yellow = S). (For interpretation of the references to colour in this figure legend, the reader is referred to the web version of this article.)

Table 3
Gibbs free energies of reaction for the four steps scheme, in kcal/mol at 333 K.

	Step 1a	Step 1b	Step 2b	Step 2b
Th	−5.59	9.18	−15.93	6.75
25DMT	−10.16	8.11	−13.23	0.66
BT	−10.00	7.17	−9.33	−0.82
2MBT	−10.25	7.47	−10.04	−0.94
4MBT	−10.60	7.33	−8.83	−1.96
DBT	−12.27	5.46	−7.21	−3.06
24DMBT	−11.71	8.28	−10.06	−1.66
46DMDBT	−12.50	5.90	−7.83	−3.84

Table 4
Gibbs free energy of activation (kcal/mol) and rate constants for the different steps of the ODS process involving B1 and DBT at 333 K.

	$\Delta G^{\neq}$	k	
Step 1a	4.40	1.12E+09	$M^{-1}\,s^{-1}$
Step 2b	23.64	2.38E−03	s^{-1}
Step 2a	6.63	1.00E+09	$M^{-1}\,s^{-1}$
Step 2b	13.37	1.30E+04	s^{-1}

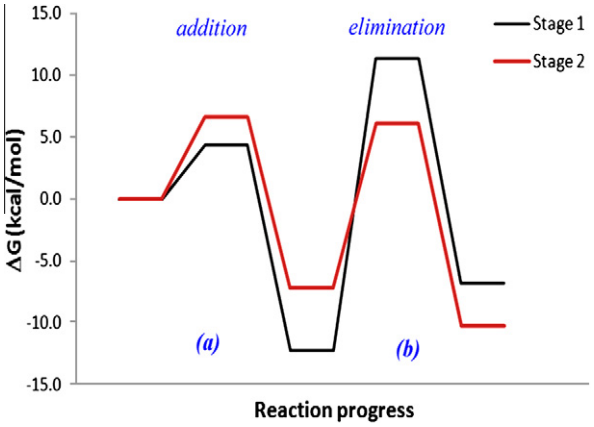

Fig. 5. Reaction profile for the ODS process involving B1 and DBT.

hypothesis that this is the rate-determining step of the ODS process. The calculated rate constant for this step was found to be $2.38 \times 10^{-3}\ s^{-1}$, which is in excellent agreement with the experimental value $7.3 \times 10^{-4}\ s^{-1}$. In fact, the calculated constant is only 3.2 times larger than that obtained from the experiments. This agreement validates not only the above-proposed hypothesis but also the reliability of the performed calculations.

It is also notable to observe the correlation obtained between the Gibbs free energy of reaction step 1b and the experimental rate constants. In Fig. 6, plots of both parameters are shown simultaneous for each model molecule.

Even though the Eyring equation (1) establishes a direct relationship between the Gibbs free energy of activation and the rate constant, the Bell–Evans–Polanyi principle also establishes a linear relation between the activation energy (Ea) and enthalpy of reaction (ΔHr) within a series of closely related chemical processes:

$$Ea = A + B\Delta Hr \tag{5}$$

In the studied case, the rate-determining step is of similar nature for all sulfur compounds, i.e., an elimination step. Therefore, the entropy change associated with this step is expected to be similar for all of them, and the Bell–Evans–Polanyi principle is fulfilled. The simultaneous manifestation of this principle and the Eyring equation justifies the correlation observed in Fig. 6. This correlation

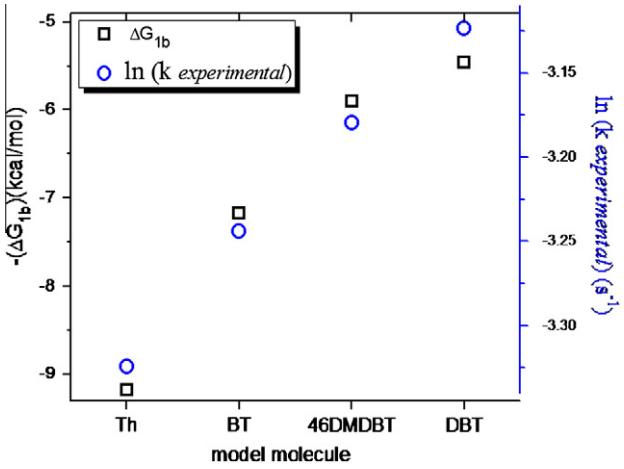

Fig. 6. Correlation between the Gibbs free energy of reaction for the step 1b (highest energy barrier) and the experimental reaction constants. Note that the parameters are expressed as ln ($k_{experimental}$) and the negative value of Gibbs energy of reaction.

between the experimental k and the calculated ΔG_{1b} strongly supports the proposed mechanism and the identification of the rate-determining step.

3.2.3. Reactivity Indexes analyses

The theoretical analysis was extended to global reactivity indexes due to their potential impact in estimating the physicochemical behavior of these model molecules.

They were calculated from vertical ionization energies (I) and vertical electron affinities (A), which were computed according to:

$$I = E^X_{n-1}(g_n) - E^X_n(g_n) \tag{6}$$

$$A = E^X_n(g_n) - E^X_{n+1}(g_n) \tag{7}$$

where $E^X_n(g_n)$ is the energy of the n-electron system calculated at the optimized geometry g_n and $E^X_{n-1}(g_n)$ and $E^X_{n+1}(g_n)$ are the energies of the $(n-1)$-electron and $(n+1)$-electron species calculated at the g_n geometry. Since the reactivity indexes are obtained from I and A values, their accuracy would be determined by those of I and A. Therefore, a comparison between calculated and experimental values of I and A has been performed in order to test the reliability of the present calculations (Table 1S).

The analyzed reactivity indexes are hardness (η), electrophilicity (ω), electroaccepting power (ϖ^+), and electrodonating power (ϖ^-). The absolute hardness plays an important role in Pearson's hard and soft acids and bases (HSAB) [45–47] and maximum hardness principles (MHP) [47,48]. It is defined as the second derivative of the electronic energy of the system with respect to the number of electrons, at a constant external potential [49]:

$$\eta = \frac{1}{2}\left(\frac{\partial^2 E}{\partial N^2}\right)_{v(r)} \tag{8}$$

It can be evaluated, based on the commonly used finite difference approximation, as:

$$\eta = I - A \tag{9}$$

and represents the resistance of a chemical species to change its number of electrons or the shape of its electron cloud.

Electrophilicity is also a very important global reactivity descriptor since its value would determine the chemical behavior of the reacting species, i.e., when comparing different species that can act as electrophile, as it is expected to be the case of the sulfur

compounds in the reactions studied in this work, the one with the highest electrophilicity is expected to be the most reactive one. In this work, ω has been calculated as:

$$\omega = \frac{(I+A)^2}{8(I-A)} \tag{10}$$

as proposed by Parr et al. [50] for the ground-state parabola model.

Electroaccepting and electrodonating powers, which have been recently presented by Gazquez et al. [51], are ideal for describing the propensity of a given chemical species to donate or accept fractional amounts of charge. They are expected to show a similar behavior to that of the first ionization potential and the electron affinity, respectively. However, while I and A measure the capability of a chemical system to donate or accept one electron, ϖ^+ and ϖ^- measure the capability of a chemical system to donate or to accept a small fractional amount of charge [52]. They have been calculated as:

$$\varpi^+ = \frac{(I+3A)^2}{16(I-A)} \tag{11}$$

$$\varpi^- = \frac{(3I+A)^2}{16(I-A)} \tag{12}$$

The values of the ionization energies, electron affinities, hardness, electrophilicity, electrodonating power, and electroaccepting power for the studied sulfur compounds are reported in Table 5. As these values show the trends described above, concerning the thermochemical feasibility of the first stage of the ODS process correlates well with the values of η, ϖ^-, and ϖ^+. The compounds with the lower hardness (DBT and 46DMDBT) are those leading to the most negative values of Gibbs free energies of reaction, while those with the highest hardness (Th and 25DMT) correspond to the least thermodynamically favored reactions.

At this point, it seems important to keep in mind that since charge acceptance processes stabilize the system, larger values of ϖ^+ imply a larger capability to accept electrons. Charge donating processes, on the other hand, destabilize the system, and therefore, smaller values of ϖ^- indicate a larger capability to donate electrons [52] Therefore, and according to the values of ϖ^- and ϖ^+ reported in Table 5, DBT and 46DMDBT have the largest capability to accept electrons and the lowest capability to donate electrons. 25DMT and Th, on the other hand, have the lowest capability to accept electrons and the largest capability to donate electrons. Therefore, it can be inferred that in the first stage of the ODS process, the charge transfer takes place from the peroxo-complex toward the sulfur compound. This seems coherent with the fact that the oxygen atoms in the peroxo-group of the catalyst are negatively charged, while the S atoms in the sulfur compounds are positively charged. Therefore, the computed reactivity indexes provide an explanation to the thermochemical feasibility of the different modeled reactions.

Table 5
Ionization energies (I), electron affinities (A), hardness (η), electrophilicity (ω), electrodonating power (ϖ^-), and electroaccepting power (ϖ^+), in eV, for the studied sulfur compounds.

	I	A	η	ω	ϖ^-	ϖ^+
Th	6.55	0.99	5.57	1.28	4.78	1.02
25DMT	6.03	0.90	5.13	1.17	4.39	0.92
BT	6.11	1.34	4.77	1.45	5.07	1.34
2MBT	6.03	1.30	4.73	1.42	4.97	1.31
4MBT	6.05	1.31	4.74	1.43	4.99	1.31
DBT	6.05	1.66	4.38	1.70	5.59	1.74
24DMBT	5.97	1.28	4.69	1.40	4.91	1.28
46DMDBT	5.97	1.56	4.41	1.61	5.37	1.61

Since, as discussed above, the first stage of the ODS process seems to be the most difficult to accomplish from a thermochemical point of view, it is proposed that structures resembling clusters B1 and Eb would favored the desired reactions. When these structures are involved, both stages of reaction were found to be exergonic for all the studied sulfur compounds but Th. For the latter, the first stage of the ODS was found to be endergonic, regardless of the structure of the active site in the catalyst. However, even for thiophene, the sum of the Gibbs free energies of the two stages leads to a negative overall Gibbs free energy. Regarding the sulfur compounds, it is predicted that the reactions involving DBT and 46DMDBT would lead to the largest energy release. However, since both stages of the ODS process (and the overall Gibbs free energy of reaction) were found to be significant exergonic for all the studied sulfur compounds, when reacting with peroxo-complex B1 and Eb sites, such structures are predicted to efficiently accomplish oxidative desulfurization. Additionally, our results show that not all the reaction sites on the surface of peroxo-complexes domains are equally actives and predict that thermochemical feasibility strongly depend on both: chemical nature of the active sites on the catalyst and nature of the aromatic sulfur compound.

4. Conclusions

The experimental and theoretical study of the relationships between oxidative reactivity, thermochemical viability, and surface structural requirement of the active sites in oxidative desulfurization (ODS) process allows establishing the following conclusions:

The results also reveal that the ODS takes place in two stages, the formation of sulfoxide and the formation of sulfone and that each stage occur in two independent steps, addition and elimination, involving the formation of intermediate adducts. So the values of the Gibbs free energy of activation show that the barriers of the addition steps (*1a* and *2a*) are significantly lower than those of the elimination steps (*1b* and *2b*), supporting the hypothesis that the elimination is the rate-determining step of the ODS process.

The experimental oxidative reactivity evaluated as oxidation rate constants (k) decreased according to the order: $DBT > 46DMDBT > BT \gg Th$, which is related to the electron density on the sulfur atoms.

The reactivity indexes of the studied sulfur compounds provide an explanation to the thermochemical feasibility of the ODS process and confirm that the thermochemistry of the reaction depends on both: the structural characteristic of the surface sites and the nature of the aromatic sulfur compounds.

The oxidized products of DBTs and BT were experimentally identified as the corresponding sulfones, while sulfoxides were not detected as products. In the case of thiophene, the reaction yielded H_2SO_4 and thiophene sulfoxide, while thiophene sulfone was not detected. This has been explained based on the structural features of the thiophene sulfone, obtained from calculations. All this supports that the products arising from oxidation reactions would be dependent on the nature of the reacting sulfur compound.

The thermochemical study indicates that the sulfone formation (stage 2) is most favored than the sulfoxide formation (stage 1) and supports the experimental evidence that ODS reactions involving DBT and 46DMDBT are particularly favored, compared to those involving other sulfur compounds.

Thermochemical feasibility and global reactivity indexes computed for different sulfur compounds indicates that the ODS reactivity decreases in the following order: $DBT > 46DMDBT > 24DMBT > 4MBT \sim BT \sim 2MBT \sim 25DMT \gg Th$. This trend confirms that the reactivity of the sulfur compounds correlate well with their electronic properties, such as: η, ϖ^-, and ϖ^+ and that

dibenzothiophene (DBT), alkyl-substituted sulfur compounds, especially 4,6-dimentyldibenzothiophene (46-DMDBT), are particularly reactive in the oxidation reactions.

Acknowledgments

A. G. thanks Laboratorio de Visualización y Cómputo Paralelo at UAM – Iztapalapa for the access to its computer facilities.

Appendix A. Supplementary material

Supplementary data associated with this article can be found, in the online version, at doi:10.1016/j.jcat.2011.06.010.

References

[1] M. Houalla, D.H. Broderick, A.V. Sapre, N.K. Nag, V.H.J. De Beer, B.C. Gates, H. Kwart, J. Catal. 61 (1980) 523.
[2] C. Song, X. Ma, Appl. Catal. B: Environ. 41 (2003) 207.
[3] F.M. Collins, A.R. Lucy, C. Sharp, J. Mol. Catal. A: Chem. 117 (1997) 397.
[4] M. Te, C. Fairbridge, Z. Ring, Appl. Catal. A: Gen. 219 (2001) 267.
[5] S. Otsuki, T. Nonaka, N. Takashima, W. Qian, A. Ishihara, T. Imai, T. Kabe, Energy Fuels 14 (2000) 1232.
[6] J.M. Campos-Martin, M.C. Capel-Sanchez, P. Perez-Presas, J.L.G. Fierro, J. Chem. Technol. Biotechnol. 85 (2010) 879.
[7] C. Li, Z. Jiang, J. Gao, Y. Yang, S. Wang, F. Tian, F. Sun, X. Sun, P. Ying, C. Han, Chem. Eur. J. 10 (2004) 2277.
[8] J.M. Fraile, J.I. García, B. Lázaro, J.A. Mayoral, Chem. Commun. (1998) 1807.
[9] J.B. Gao, S.G. Wang, Z.X. Jiang, H.Y. Lu, Y.X. Yang, F. Jing, C. Li, J. Mol. Catal. A: Chem. 258 (2006) 261.
[10] H. Lü, J. Gao, Z. Jiang, F. Jing, Y. Yang, G. Wang, C. Li, J. Catal. 239 (2006) 369.
[11] H. Lü, Y. Zhang, Z. Jiang, C. Li, Green Chem. 12 (2010) 1954.
[12] F. Figueras, J. Palomeque, S. Loridant, C. Fèche, N. Essayem, G. Gelbard, J. Catal. 226 (2004) 25.
[13] D. Huang, Z. Zhai, Y.C. Lu, L.M. Yang, G.S. Luo, Ind. Eng. Chem. Res. 46 (2007) 1447.
[14] F. Al-Shahrani, T.C. Xiao, S.A. Llewellyn, S. Barri, Z. Jiang, H.H. Shi, G. Martinie, M.L.H. Green, Appl. Catal. B: Environ. 73 (2007) 311.
[15] H. Li, L. He, J. Lu, W. Zhu, X. Jiang, Y. Wang, Y. Yan, Energy Fuels 23 (2009) 1354.
[16] J.L. Garcia-Gutierrez, G.A. Fuentes, M.E. Hernandez-Teran, P. Garcia, F. Murrieta-Guevara, F. Jimenez-Cruz, Appl. Catal. A: Gen. 334 (2008) 366.
[17] H. Gómez-Bernal, L. Cedeño-Caero, A. Gutiérrez-Alejandre, Catal. Today 142 (2009) 227.
[18] E. Torres-Garcia, G. Canizal, S. Velumani, L.F. Ramirez-Verdusco, F. Murrieta-Guevara, J.A. Ascencio, Appl. Phys. A 79 (2004) 2037.
[19] A. Galano, G. Rodriguez-Gattorno, E. Torres-Garcia, Phys. Chem. Chem. Phys. 10 (2008) 4181.
[20] A. Iribarren, G. Rodriguez-Gattorno, J.A. Ascencio, A. Medina, E. Torres-Garcia, Chem. Mater. 18 (2006) 5446.
[21] P. Moreau, V. Hulea, S. Gomez, D. Brunel, F. Di Renzo, Appl. Catal. A: Gen. 155 (1997) 253.
[22] L. Cedeño-Caero, E. Hernandez, F. Pedraza, F. Murrieta, Catal. Today 107–108 (2005) 564.
[23] V. Hulea, F. Fajula, J. Bousquet, J. Catal. 198 (2001) 179.
[24] A. Ishihara, D. Wang, F. Dumeignil, H. Amano, E.W. Qian, T. Kabe, Appl. Catal. A: Gen. 279 (2005).
[25] Gaussian 03, Revision E.01, M.J. Frisch, G.W. Trucks, H.B. Schlegel, G.E. Scuseria, M.A. Robb, J.R. Cheeseman Jr., J.A. Montgomery, T. Vreven, K.N. Kudin, J.C. Burant, J.M. Millam, S.S. Iyengar, J. Tomasi, V. Barone, B. Mennucci, M. Cossi, G. Scalmani, N. Rega, G.A. Petersson, H. Nakatsuji, M. Hada, M. Ehara, K. Toyota, R. Fukuda, J. Hasegawa, M. Ishida, T. Nakajima, Y. Honda, O. Kitao, H. Nakai, M. Klene, X. Li, J.E. Knox, H.P. Hratchian, J.B. Cross, V. Bakken, C. Adamo, J. Jaramillo, R. Gomperts, R.E. Stratmann, O. Yazyev, A.J. Austin, R. Cammi, C. Pomelli, J.W. Ochterski, P.Y. Ayala, K. Morokuma, G.A. Voth, P. Salvador, J.J. Dannenberg, V.G. Zakrzewski, S. Dapprich, A.D. Daniels, M.C. Strain, O. Farkas, D.K. Malick, A.D. Rabuck, K. Raghavachari, J.B. Foresman, J.V. Ortiz, Q. Cui, A.G. Baboul, S. Clifford, J. Cioslowski, B.B. Stefanov, G. Liu, A. Liashenko, P. Piskorz, I. Komaromi, R.L. Martin, D.J. Fox, T. Keith, M.A. Al-Laham, C.Y. Peng, A. Nanayakkara, M. Challacombe, P.M.W. Gill, B. Johnson, W. Chen, M.W. Wong, C. Gonzalez, J.A. Pople, Gaussian, Inc., Wallingford CT, 2004.
[26] J.P. Perdew, K. Burke, Y. Wang, Phys. Rev. B 54 (1996) 16533. and references therein.
[27] T.H. Dunning Jr., P.J. Hay, Modern Theoretical Chemistry, in: H.F. Schaefer III (Ed.), vol. 3, Plenum, New York, 1976.
[28] L.v. Szentpaly, P. Fuentealba, H. Preuss, H. Stoll, Chem. Phys. Lett. 93 (1982) 555.
[29] H. Stoll, P. Fuentealba, P. Schwerdtfeger, J. Flad, L.v. Szentpaly, H. Preuss, J. Chem. Phys. 81 (1984) 2732.
[30] P. Fuentealba, H. Preuss, H. Stoll, L.v. Szentpaly, Chem. Phys. Lett. 89 (1989) 418.
[31] M.T. Cances, B. Mennucci, J. Tomasi, J. Chem. Phys. 107 (1997) 3032.
[32] B. Mennucci, J. Tomasi, J. Chem. Phys. 106 (1997) 5151.
[33] B. Mennucci, E. Cances, J. Tomasi, J. Phys. Chem. B 101 (1997) 10506.
[34] J. Tomasi, B. Mennucci, E. Cances, THEOCHEM 464 (1999) 211.
[35] H. Eyring, J. Chem. Phys. 3 (1935) 107.
[36] M.G. Evans, M. Polanyi, Trans. Faraday Soc. 31 (1935) 875.
[37] D.G. Truhlar, W.L. Hase, J.T. Hynes, J. Phys. Chem. 87 (1983) 2664.
[38] F.C. Collins, G.E. Kimball, J. Colloid Sci. 4 (1949) 425.
[39] M. Smoluchowski, Z. Phys. Chem. 92 (1917) 129.
[40] (a) A. Einstein, Ann. Phys. (Leipzig) 17 (1905) 549;
(b) G.G. Stokes, Mathematical and Physical Papers, vol. 3, Cambridge University Press, Cambridge, 1903. esp. Sect. IV, p. 55.
[41] L.F. Ramirez-Verduzco, E. Torres-Garcia, R. Gomez-Quintana, V. Gonzalez-Pena, F. Murrieta-Guevara, Catal. Today 98 (2004) 289.
[42] G. Rodriguez-Gattorno, A. Galano, E. Torres-Garcia, Appl. Catal. B: Environ. 92 (2009) 1.
[43] A. Milenkovic, E. Schulz, V. Meille, D. Loffreda, M. Forissier, M. Vrinat, P. Sautet, M. Lemaire, Energy Fuels 13 (1999) 881.
[44] Y. Shiraishi, K. Tachibana, T. Hirai, I. Komasawa, Ind. Eng. Chem. Res. 41 (2002) 4362.
[45] R.G. Pearson, J. Am. Chem. Soc. 85 (1963) 3533.
[46] R.G. Pearson, Science 151 (1966) 172.
[47] R.G. Pearson, Chemical Hardness, John Wiley and Sons, New York, 1997.
[48] R.G. Pearson, Acc. Chem. Res. 26 (1993) 250.
[49] R.G. Parr, R.G. Pearson, J. Am. Chem. Soc. 105 (1983) 7512.
[50] R.G. Parr, L.v. Szentpaly, S. Liu, J. Am. Chem. Soc. 121 (1999) 1922.
[51] J.L. Gazquez, A. Cedillo, A. Vela, J. Phys. Chem. A 111 (2007) 1966.
[52] J.L. Gázquez, J. Mex. Chem. Soc. 52 (1) (2008) 3.